Optimal Design of AC EMI Filters with Damping Networks and Effect on the System Power Factor

Nico Hensgens, Marcelo Silva,
Jesús A. Oliver, José A. Cobos

Stanislav Skibin, Andreas Ecklebe

***Abstract*—The cutoff frequencies of an EMI filter are normally given by the noise attenuation requirements the filter has to fulfill. In order to select the component values of the filter elements, i.e. inductances and capacitances, an additional design criterium is needed. In this paper the effect of the EMI filter input and output impedances are considered. The input impedance influences the filters effect on the system displacement power factor and the output impedance plays a key role in the system stability. The effect of filter element values, the number of filter stages as well as additional damping networks are considered and a design procedure is provided. For this analysis a two-port description of the input filters employing $ABCD$-parameters is used.**

***Index Terms*—EMI, EMC, input filter, damping, power factor, optimization**

I. Introduction

Power converters are sources of conducted and radiated electromagnetic interferences (EMI) [1],[2] and international standards have been established specifying the maximal limits depending on the area of application [3],[4],[5]. In order to comply with these standards, generally an input filter is required.

The attenuation requirement of the filter can be obtained by comparing the noise emissions with the applicable standard. Based on this attenuation requirement, the filter cutoff frequency of an LC filter stage can be selected. The filter components can be designed in order to optimize the input filter w.r.t. some characteristic or fitness function. This function can be a combination of different criteria, e.g. weight, volume, losses, etc. [18]. In order to find the values of the individual filter elements an additional design criterium is needed. In [7] a filter design procedure for AC line applications has been presented, however no clear statement on how to select the component values of L and C has been provided. In [6] another filter design procedure for power factor correction (PFC) circuits has been presented, including the effect of the input filter on the system power factor as well as damping considerations. However this paper focussed on the rather uncommon Chebyshev filter topology and the effect of the damping networks on the distortion of the power factor has not been considered in detail. In the present paper two distinct selection criteria for the filter components are analyzed; these are the effect of the input filter components on the filter input impedance Z_{in} and output impedance Z_{out}. The input impedance being related to the displacement power factor ($DPF = \cos\phi$ (ϕ being the displacement angle between input voltage and current)) of the system, and the output impedance playing an import role in system stability considerations.

II. Input Filter Description

In this work $ABCD$-parameters are used to provide a framework for the analytical description of input filters and the calculation of all necessary impedances, e.g. input impedance Z_{in} and output impedance Z_{out}. A general two-port network is shown in Fig. 1. The input and output variables of the system are V_1, I_1 and V_2, I_2 respectively. The $ABCD$-parameter

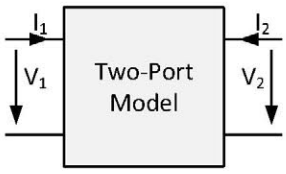

Fig. 1. General two-port model with definition of input and output current and voltage references

description of the two-port network in Fig. 1 is as follows:

$$\begin{pmatrix} V_1 \\ I_1 \end{pmatrix} = \begin{pmatrix} A & B \\ C & D \end{pmatrix} \cdot \begin{pmatrix} V_2 \\ -I_2 \end{pmatrix} \tag{1}$$

This description method allows to calculate the $ABCD$-matrix of a cascaded system, by multiplication of the matrices of the individual sub-systems in the same order as they would be drawn in a network diagram and also connected in reality.

The input and output impedances Z_{in} and Z_{out} of the network, as defined in Figs. 3 and 4, can be calculated as

$$Z_{in} = \frac{A}{C} \tag{2}$$

$$Z_{out} = \frac{B}{A} \tag{3}$$

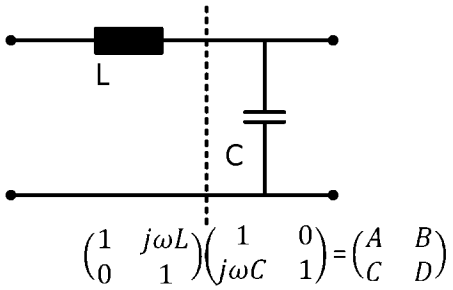

Fig. 2. Two-port employing $ABCD$-parameters of a single-stage LC filter with resistive load

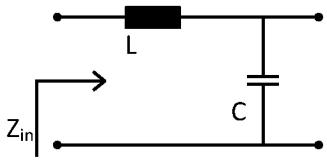

Fig. 3. Input impedance definition of an LC filter

As an example a single-stage LC filter is shown in Fig. 2. For this network, the $ABCD$-matrix is

$$\begin{pmatrix} A & B \\ C & D \end{pmatrix} = \begin{pmatrix} 1-\omega^2 LC & j\omega L \\ j\omega C & 1 \end{pmatrix} \tag{4}$$

and the the input and output impedances result in

$$Z_{in} = \frac{A}{C} = \frac{1-\omega^2 LC}{j\omega C} \tag{5}$$

$$Z_{out} = \frac{B}{A} = \frac{j\omega L}{1-\omega^2 LC} \tag{6}$$

III. Filter Design and DPF Variation

A. LC Filter Design Procedure

For a simple LC filter the following relationships between the required attenuation att (in $dB\mu V$) at a specific frequency f_{att} (in Hz), the cutoff frequency f_c and the product $L \cdot C$ of the two filter elements, i.e. the inductance L and the capacitance C can be used [19].

$$f_c = \frac{f_{att}}{\sqrt{10^{att/20}}} = \frac{1}{2\pi LC} \tag{7}$$

These provide the product value LC as a function of att and f_{att}.

$$LC = \frac{10^{att/20}}{f_{att}^2} \tag{8}$$

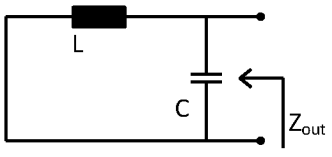

Fig. 4. Output impedance definition of an LC filter

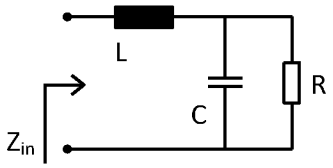

Fig. 5. LC filter with resistive load

Note that the single LC filter can be a single stage of a multi-stage filter topology where att denotes the attenuation this individual filter stage needs to provide. There is a degree of freedom in selecting the individual values of the inductance L and the capacitance C. The values of L and C can be selected in order to comply with some additional design criterium, e.g. regarding DPF variation or minimal output impedance. These criteria will be discussed in the following sections.

B. Single stage with resistive load

The simplest possible case which we will consider in this section is a single-stage LC filter with a resistive load R_L as shown in Fig. 5. The resistive load could for example be a simple model of a PFC converter providing a zero degree phase shift between input voltage and input current.

The input impedance of this network is given by:

$$Z_{in} = \frac{R}{1+\omega^2 C^2 R^2} + j\left(\omega L - \frac{\omega C R^2}{1+\omega^2 C^2 R^2}\right) + \tag{9}$$

The combinations of L and C resulting in a phase angle of zero, i.e. resistive Z_{in} and unitary DPF, are shown in Fig. 6. Figs. 6(a) and 6(b) show curve families in the $L-C$-plane which lead to a unity DPF for different values of the resistive load R ($R = 0.1 : 0.1 : 10\Omega$) and for grid frequencies of $50Hz$ and $400Hz$ respectively. Figs. 6(c) and 6(d) depict one case ($R = 3\Omega$), the same as Figs. 6(e) and 6(f). One can see in these figures how the DPF varies depending on the values for L and C and that it is more sensitive to variations in the components values for higher grid frequencies.

In [17] and [18] is has been shown that in order to obtain a filter not influencing the DPF, i.e. an input impedance Z_{in} with resistive characteristic, the filter components L and C should be selected as follows:

$$C = \frac{1}{R\sqrt{\omega_c^2 - \omega_g^2}} = \frac{1}{R\omega_c\sqrt{1-\left(\frac{\omega_g^2}{\omega_c^2}\right)}} \tag{10}$$

$$L = \frac{1}{\omega_c^2 C_d} \tag{11}$$

Where ω_c is the cutoff frequency of the LC filter stage, ω_g is the grid frequency and C_d is the commercially available capacitance value, closest to the value C. As long as the grid-frequency ω_g is small compared to the cutoff frequency ω_c of the filter , the effect of the input filter on the power factor is limited. However the closer ω_c and ω_g get together the more the effect on the DPF needs to be considered. This might be

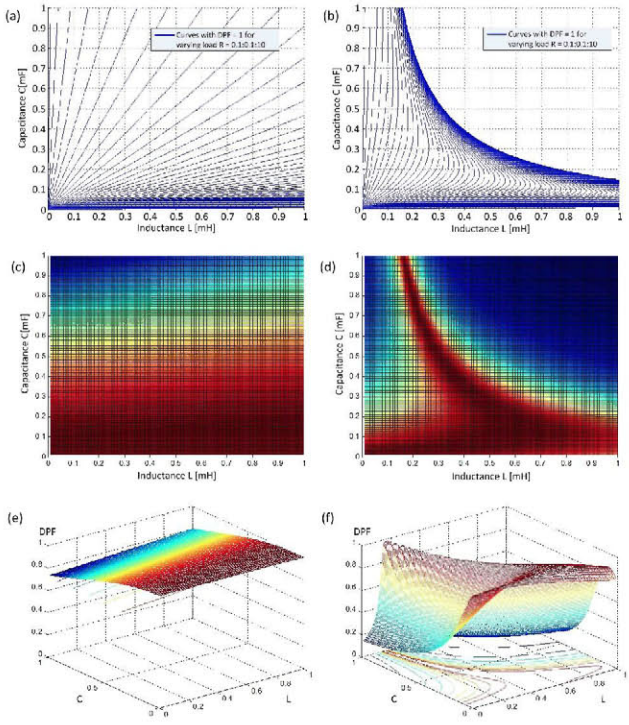

Fig. 6. Set of curves of combinations of L and C providing unity DPF for grid frequencies of $50Hz$ (a) and $400Hz$ (b) and varying resistive load; DPF as a function of L and C for one specific load R in the cases of grid frequencies of $50Hz$(c),(e) and $400Hz$ (d),(f).

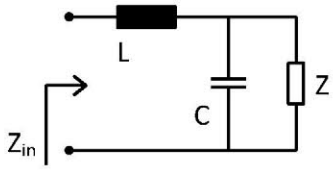

Fig. 7. LC filter with general complex load

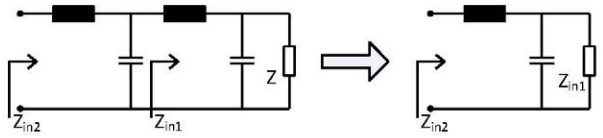

Fig. 8. Simplification of a two-stage LC filter structure with general load Z into a single-stage LC filter

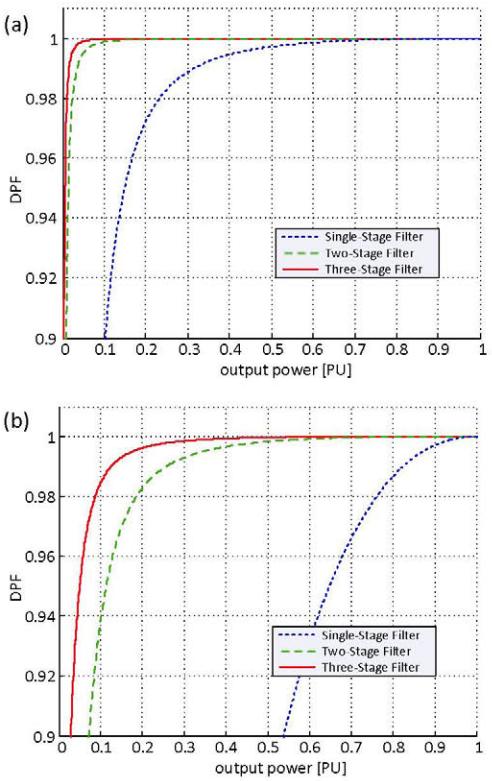

Fig. 9. DPF a single-stage, two-stage and three-stage filters designed for unity DPF at maximal output power, as a function of the output power, for grid frequencies of $50Hz$ (a) and $400Hz$ (b)

the case when using a very low cutoff frequency of the input filter is chosen, e.g. in case of a single-stage topology, or in case of a high grid-frequency, e.g. in aerospace applications where grid-frequencies of up to 800 Hz are in use.

C. Single filter stage with complex load

In case the converter cannot be modeled as a simple resistor, but a more complicated model needs to be used, the previous considerations need to be extended. The resistive load model R can be replaced by a general complex frequency-dependent impedance $Z = Z_r(\omega) + jZ_i(\omega)$, as shown in Fig. 7. The input impedance of this circuit consisting of the complex load Z together with an LC filter can then be calculated, similar to (9). By setting the imaginary part of this input impedance to zero for a specific operating point, one obtains the conditions for selecting the values of L and C for unity DPF.

D. Multi-stage filter design considerations

In case the filter consists of multiple stages the calculation of L and C of the individual filter stages can be done independently by replacing the load impedance together with a first filter stage by an equivalent impedance, as shown in Fig. 8. Note that in case the first filter stage has been designed using the aforementioned approach for unity DPF, the resulting equivalent impedance should be resistive.

Figs. 9(a) and 9(b) depict the DPF of a system, consisting of a resistive load with one, two and three filter stages connected at its input as a function of the processed power. The filters have been designed in order to have unity DPF at the rated power. Fig. 9(a) shows the case of a 50 Hz grid frequency and Fig. 9(b) the case for a grid frequency of 400 Hz. One can see that the effect of the input filter on the DPF increases and becomes significant when the converter operates

much below its nominal power level due to the proportionally higher part of reactive energy in the filter passive components. One can also see that the effect can be considerably reduced by employing multi-stage filter topologies, e.g. two- or three-stage filters. This can be explained by the smaller filter component values and the resulting smaller reactive powers flowing. In general one can state that in order to keep a minimal effect of the input filter on system DPF, the size of the reactive filter elements needs to be limited.

IV. Output Impedance and Damping Networks

In the previous section the influence of the input filter on the DPF has been considered to select values for the filter inductance L and the filter capacitance C. Another criterium which normally needs to be considered is the system stability performance [12],[13], which is satisfied if the output impedance of the input filter is lower than the converter input impedance.

According to [11] we define Z_N as the converter input impedance under the condition that its feedback controller operates ideally, i.e. varies the duty-cycle in such a way that the output voltage variations are null and Z_D as the converter input impedance under the condition that the duty-cycle variations by the controller are null. Then the stability criteria can be written as:

$$|Z_{out}| \ll |Z_N| \tag{12}$$

$$|Z_{out}| \ll |Z_D| \tag{13}$$

In order to comply with the above mentioned stability criteria, the output impedance of the input filter needs to be limited. To achieve this, two different aspects need to be considered. First the asymptotic output impedance of the input filter needs to be reduced to a sufficient level by increasing the filter capacitance C. In a second approach damping networks [10],[15],[14] need to be employed in order to damp the output impedance peak at the filter resonance frequency.

A. Filter output impedance

Fig. 10 shows a general output impedance of an LC filter. The asymptotic output impedance is shown which has a maximum value R_0 at the filter resonance frequency f_0, as well as the real output impedance characteristic, which peaks at that same frequency.

In Fig. 11 the (asymptotic as well as real) output impedances of five different filters are shown. All filters have the same cutoff/resonance frequencies, i.e. have the same product of inductance L and capacitance C and thus provide the same noise attenuation. However they are all implemented using different combinations of L and C. One can clearly observe that the individual values of L and C have a significant influence on the filter output impedance and thus need to be considered when trying to comply with the above mentioned stability criterium. In order to reduce the asymptotic output impedance, the capacitance should be selected as big as possible and the inductance value as small as possible. A bigger capacitance however causes the flow of large reactive currents and thus a lower DPF.

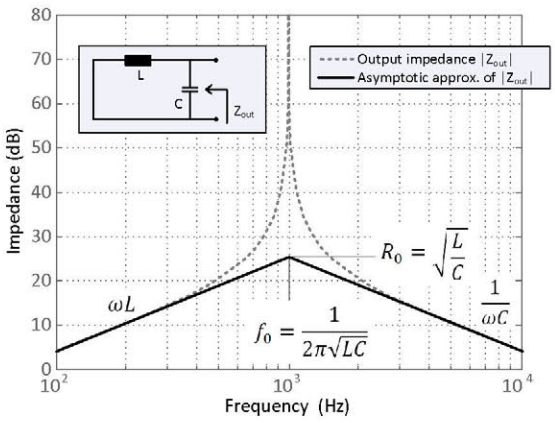

Fig. 10. Output impedance characteristic of a generic LC filter consisting of an inductance L and a capacitance C. The resonance frequency is f_0 and the asymptotic peak impedance is R_0

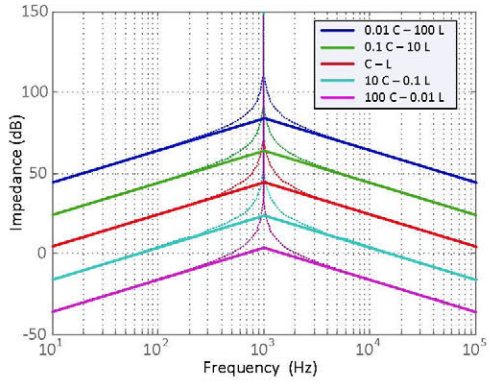

Fig. 11. Asymptotic and real output impedance characteristics of five different filters, providing the same cutoff frequency and attenuation characteristics but implemented using different combinations of inductance L and capacitance C. It can be seen that filters employing a larger C and smaller L provide a lower/better output impedance than filters employing a small C and a large L

B. Damping Networks

In Fig. 12 the three standard damping networks, employing a single damping resistor are shown. The three networks are denoted series-RL (cf. Fig. 12(a)), parallel-RL (cf. Fig. 12(b)) and parallel-RC (cf. Fig. 12(c)) damping networks.

The input impedance Z_{in} and output impedance Z_{out} of the three damping networks can be calculated using the $ABCD$-parameters and the optimal resistor dimensioning methods, presented in [10].

- Series-RL damping

In case of the series-RL damping network from Fig. 12(a), the relevant impedances can be calculated using the multiplication

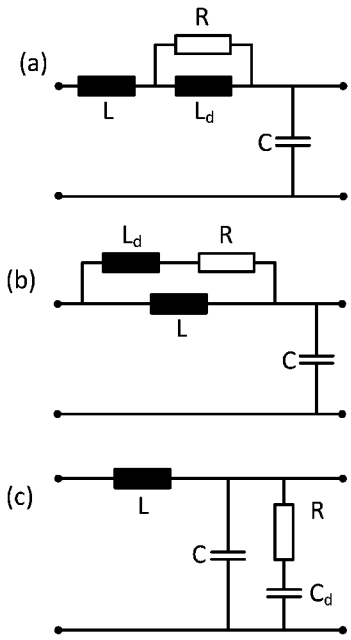

Fig. 12. Single resistor damping networks: series-RL (a), parallel-RL (b) and parallel-RC (c)

of the individual ABCD matrices of the filter components:

$$ABCD_{RL_s} = \begin{pmatrix} 1 & j\omega L \\ 0 & 1 \end{pmatrix} \begin{pmatrix} 1 & \frac{j\omega L_d R}{j\omega L_d + R} \\ 0 & 1 \end{pmatrix} \begin{pmatrix} 1 & 0 \\ j\omega C & 1 \end{pmatrix} \tag{14}$$

with the damping factor n defined as

$$L_d = n \cdot L \tag{15}$$

and

$$R_d = \sqrt{\frac{L}{C}} \left(\frac{n}{n+1} \right) \sqrt{\frac{(2+n)(4+3n)}{2(1+n)(4+n)}} \tag{16}$$

- Parallel-RL damping

In case of the parallel-RL damping network from Fig. 12(b), the relevant impedances can be calculated using

$$ABCD_{RL_s} = \begin{pmatrix} 1 & \frac{j\omega L(j\omega L_d + R)}{j\omega L + j\omega L_d + R} \\ 0 & 1 \end{pmatrix} \begin{pmatrix} 1 & 0 \\ j\omega C & 1 \end{pmatrix} \tag{17}$$

with

$$L_d = n \cdot L \tag{18}$$

and

$$R_d = \sqrt{\frac{L}{C}} \sqrt{\frac{n(3+4n)(1+2n)}{2(1+4n)}} \tag{19}$$

- Parallel-RC damping

In case of the parallel-RC damping network from Fig. 12(c), the relevant impedances can be calculated using

$$ABCD_{RC_p} = \begin{pmatrix} 1 & j\omega L \\ 0 & 1 \end{pmatrix} \begin{pmatrix} 1 & 0 \\ j\omega C & 1 \end{pmatrix} \begin{pmatrix} 1 & 0 \\ \frac{j\omega C_d}{1 + j\omega R C_d} & 1 \end{pmatrix} \tag{20}$$

with the damping factor n defined as

$$C_d = n \cdot C \tag{21}$$

and

$$R_d = \sqrt{\frac{L}{C}} \sqrt{\frac{(2+n)(4+3n))}{2n^2(4+n)}} \tag{22}$$

In Fig. 13 the effect of the damping factor n on the filter output impedance is shown, for all three different damping networks and for different values of n. The arrow indicates the sense of increasing n in the curve families, and the highlighted curve in black shows the case for $n = 1$. When designing the damping network, the damping factor n needs to be selected in such a way that the resonance peak in the filter output impedance does not reach the level of the input impedance of the system it is connected to. In most cases, a value of $n \sim 1$ is a reasonable choice, providing adequate damping of the resonance peak while not leading to prohibitively large damping elements. We can see in Fig. 13 that in the case of $n = 1$, Z_{out} is around $10dB\mu V$ above the peak of the asymptotic output impedance which would be $0dB\mu V$ for the example curves shown in Fig. 13. This overshoot can be considered in the filter design procedure by adding an additional margin of at least $10dB\mu V$ to the maximal asymptotic peak output impedance of the filter to be designed.

The effect of the damping networks on the DPF is shown in Fig. 14. The figures in the three rows correspond to series-RL, parallel-RL and parallel-RC damping networks respectively, the figures in the left column correspond to a grid frequency of $50Hz$ and the ones in the right column to a grid frequency of $400Hz$. The filter used in this exemplary figures has a very low cutoff frequency of $1kHz$ in order for the effects of the damping networks to become more emphasized and better appreciable. One can see in the figures that in general the effect of the additional damping network on the DPF variation by the input filter is quite small and is needs only to be considered in case the grid frequency and the filter cutoff frequency are very close together (less than one decade) and for a large damping factor n.

This leads us to the conclusion that during the filter design, when considering only the effect of the filter on the DPF, the damping network can be added in a final step to the previously designed input filter without having to worry about a large effect on the DPF.

V. Filter Design Procedure

The filter design and optimization procedure with the individual design steps is summarized in the flowchart in Fig. 15.

Before starting the design process, the required attenuation att at the frequency f_{att} needs to be known, as well as the converter input impedance. The filter cutoff frequency can be calculated (step 1) and based on (10) and (11) the values for L and C with minimal effect on the DPF can be calculated (step 2). The output impedance of the filter can be calculated and compared to the converter input impedance considering

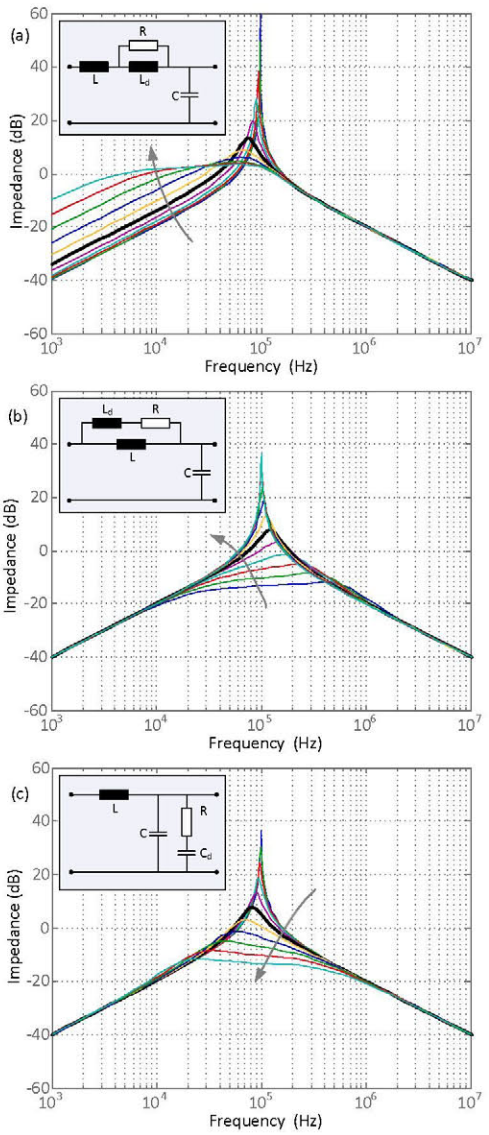

Fig. 13. Output impedance of a generic LC filter with series-RL (a), parallel-RL (b), and parallel-RC (c) damping networks. The curve sets denote the output impedance for damping factor $n = 0.03125, 0.0625, 0.125, 0.25, 0.5, 1, 2, 4, 8, 16, 32\}$, the grey arrow shows the sense of increasing n and the case of $n = 1$ is highlighted in black in all three cases.

an additional margin (step 3 and 4). If the asymptotic output impedance is lower than the system input impedance one can immediately continue with the design of a damping network (step 8). If that condition is not fulfilled, one needs to increase the value of the capacitance C and decrease the inductance L, while keeping the product $L \cdot C$, i.e. the cutoff frequency of the filter, the same (step 5). This will lead to a decrease of the filter output impedance but also has a negative effect on the DPF due to the higher reactive power flowing through the bigger capacitance. Therefore in a next step the DPF of the system must be evaluated (step 6) and checked if it still

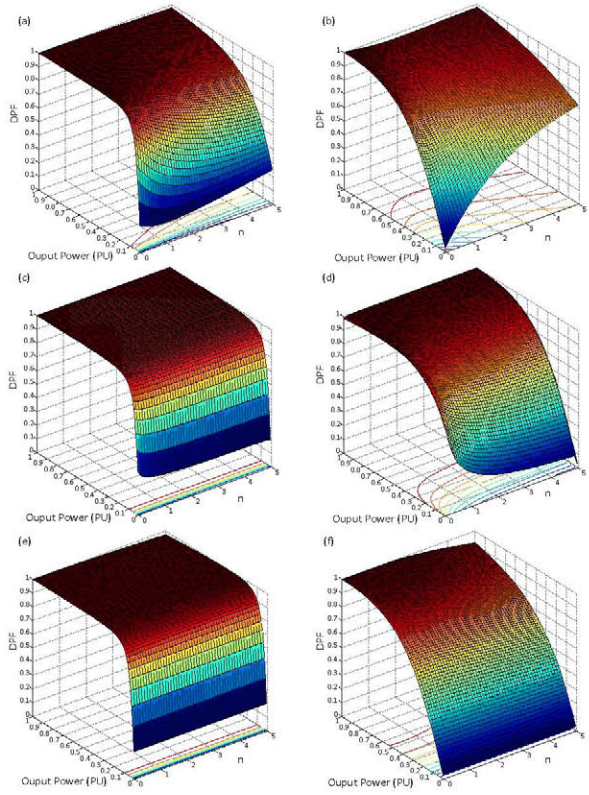

Fig. 14. Effect of damping networks on DPF for a generic LC filter with a low cutoff frequency of $1kHz$ and capacitance and inductance values selected to provide unity DPF at the rated power P_o. The figures show the cases of a grid frequency of $50Hz$ (a),(c)&(e) and $400Hz$ (b),(d)&(e). (a)&(b) show the case of series-RL damping, (c)&(d) the case of parallel-RL damping and (e)&(f) the case of parallel-RC damping.

fulfills the requirements, e.g. does meet the target of a maximal DPF variation of 5%. If the DPF is still ok, we can go back and calculate the new output impedance (step 3) and follow this loop as long as the criterium is fulfilled. If the DPF is however not ok, an additional filter stage needs to be added (step 7). This will lead to a new filter topology with a higher cutoff frequency of the individual filter stages and thus smaller reactive components and (as shown in Fig. 9) smaller effect on the DPF. How the required attenuation should be split up between the individual filter stages needs to be evaluated in a separate step.

VI. Experimental Verification

The previously discussed considerations have been evaluated in the design of the differential mode input filter for a three-phase PWM rectifier system [8],[9]. The system has an output power of $10kW$ and is operating on a $400Hz$ grid. The rectifier system is shown in Fig. 16, together with the input filter.

In Fig. 17 the schematic of the input filter is shown. It consists of a single common mode (CM) filter stage and three differential mode (DM) filter stages. The first DM filter stage (closest to the converter input) is damped using a parallel-RL

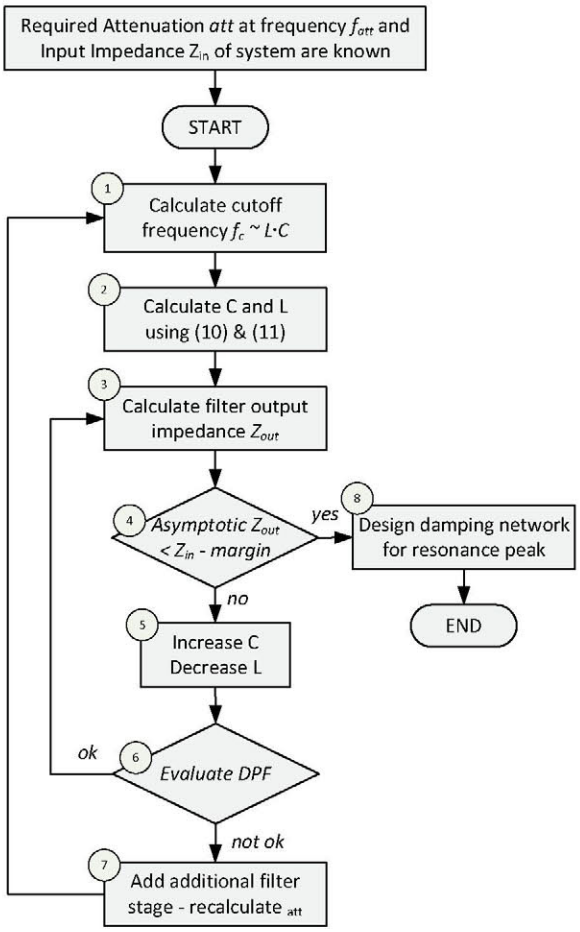

Fig. 15. Filter design flowchart.

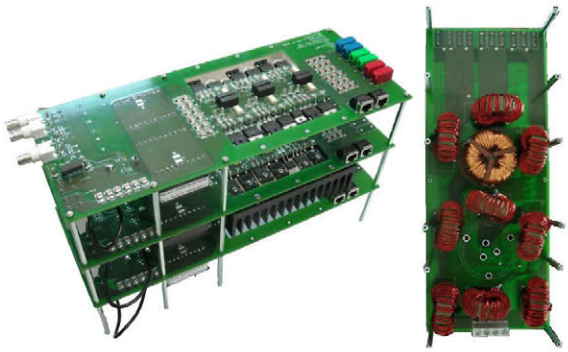

Fig. 16. Three-phase PWM rectifier (left) and input filter (right). The input filter consists of three differential-mode (DM) filter stages with parallel-RC damping networks and a single common-mode (CM) filter stage. In the picture the nine inductors of the three DM filter stages can be seen, as well as a three-phase CM choke (the PCB offers a space for a second CM choke, which is however not mounted); all filter capacitors as well as the damping capacitors and resistors are on the back-side of the filter PCB and cannot be seen in the picture.

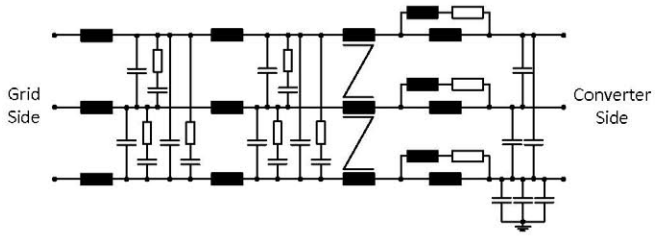

Fig. 17. Schematic of the input filter consisting of three DM filter stages and one CM filter stage. Two of the DM filter stages have parallel-RC damping and one parallel-RL damping.

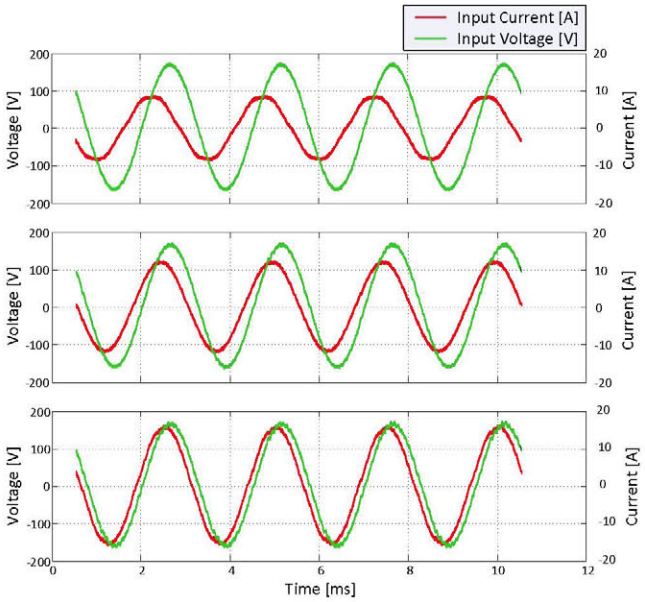

Fig. 18. Measured input voltage (green) and input current(red) waveforms of the PWM rectifier with EMI input filter and three different power levels of $11\%, 16\%$ and 21% of the maximal output power of $10kW$

damping network and the second and third DM filter stages are damped with a parallel-RC damping network.

The input voltage and current waveforms of the PWM-rectifier are shown in Fig. 18, for three different power levels. One can observe that for small power levels, the phase shift between the input current and voltage is large and it decreases with increasing power. Note that all three measurements have been performed at power levels well below the maximal rated power of the rectifier system.

Fig. 19 depicts the estimated DPF of the converter system together with the EMI input filter and the measured DPF for three power levels. The estimated curve and measured data points are in good agreement. Note that the curve of the estimated DPF is based on the designed filter as shown in Fig. 16 where the leakage inductance of the CM choke has also been considered, leading to a unity power factor at a power level around $5.5kW$.

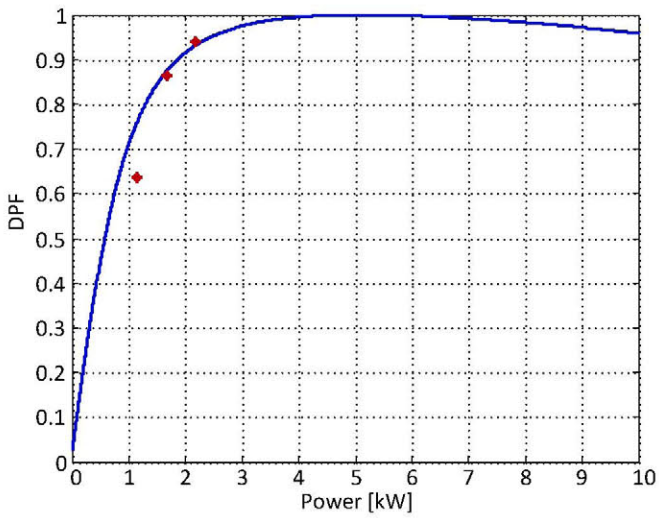

Fig. 19. Calculated DPF curve (blue) and measured DPF (red) for three different power levels. The calculated and measured data are in good agreement.

VII. Conclusions

Based on a two-prot description of the EMI input filters employing $ABCD$-parameters, the individual influences of the filter component values, i.e. sizes of the inductance L and capacitance C, the number of LC filter stages and additional damping networks on the filter input and output impedances Z_{in} and Z_{out} have been analyzed. It has been shown that multi-stage filters provide a smaller effect on the system DPF than single-stage solutions, due to the smaller size of the reactive components. Three different damping networks have been considered, these are the series-RL, parallel-RL and parallel-RC networks. It has been shown that the additional damping networks have only a limited effect on the system DPF, thus can be ignored in a first step and only be considered in a last step during filter design. A design procedure for the EMI input filter has been provided, resulting in filters with minimal effect on the system DPF while complying with system stability requirements. An experimental validation of the results has been carried out on a multi-stage input filter for a three-phase PWM rectifier system.

Acknowledgment

The authors would like to thank ABB Switzerland Ltd., Baden-Dättwil, Switzerland, for giving them the opportunity to work on this very interesting topic.

References

[1] C. R. Paul, *"Introduction to electromagnetic compatibility"*, John Wiley and Sons, 2^{nd} edition, 2006

[2] H. W.tt, *"Electromagnetic compatibility engineering"*, John Wiley and Sons, rev. edition, 2009

[3] C.I.S.P.R., *"Industrial, scientific and medical (ISM) radio-frequency equipment - electromagnetic disturbance characteristics - limits and methods of measurement", Publication 11*, Geneva, Switzerland, IEC International Special Committee on Radio Interference

[4] C.I.S.P.R., *"Information technology equipment - radio disturvbance characteristics - limits and methods of measurement", Publication 22* Geneva, Switzerland, IEC International Standard Committee on Radio Interference

[5] MIL-STD-461E, Requirements for the control of electromagnetic interference characteristics of subsystems and equipment Std., August 1999.

[6] Vlatkovic, V.; Borojevic, D.; Lee, F.C.; , "Input filter design for power factor correction circuits," Power Electronics, IEEE Transactions on , vol.11, no.1, pp.199-205, Jan 1996

[7] Fu-Yuan Shih; Chen, D.Y.; Yan-Pei Wu; Yie-Tone Chen; , "A procedure for designing EMI filters for AC line applications," Power Electronics, IEEE Transactions on , vol.11, no.1, pp.170-181, Jan 1996

[8] Dong Jiang; Rixin Lai; Fei Wang; Fang Luo; Shuo Wang; Boroyevich, D.; , "Study of Conducted EMI Reduction for Three-Phase Active Front-End Rectifier," Power Electronics, IEEE Transactions on , vol.26, no.12, pp.3823-3831, Dec. 2011

[9] Stupar, A.; Friedli, T.; Minibock, J.; Kolar, J.W.; , "Towards a 99% Efficient Three-Phase Buck-Type PFC Rectifier for 400-V DC Distribution Systems," Power Electronics, IEEE Transactions on , vol.27, no.4, pp.1732-1744, April 2012

[10] Erickson, R.W.; , "Optimal single resistors damping of input filters," Applied Power Electronics Conference and Exposition, 1999. APEC '99. Fourteenth Annual , vol.2, no., pp.1073-1079 vol.2, 14-18 Mar 1999

[11] Erickson, R.W.; Maksimovic, D.; "Fundamentals of power electronics," Springer, 2000

[12] Middlebrook, R.D.; "Input filter considerations in design and application switching regulators," IEEE Industry Applications Society Annual Meeting, 1976 Record, pp. 366-382

[13] Middlebrook, R.D.; "Design techniques for preventing input filter oscillations in switched-mode regulators," Proceedings of Powercon 5, pp. A3.1-A3.16, May 1978

[14] Lei Xing; Jian Sun; , "Optimal damping of multistage EMI filters," Power Electronics, IEEE Transactions on , vol.27, no.3, pp.1220-1227, March 2012

[15] Lei Xing; Feng, F.; Jian Sun; , "Optimal damping of EMI filter input impedance," Industry Applications, IEEE Transactions on , vol.47, no.3, pp.1432-1440, May-June 2011

[16] Cadirci, I.; Saka, B.; Eristiren, Y.; , "Practical EMI-filter-design procedure for high-power high-frequency SMPS according to MIL-STD 461," Electric Power Applications, IEE Proceedings - , vol.152, no.4, pp. 775-782, 8 July 2005

[17] Silva, M.; Hensgens, N.; Oliver, J.; Alou, P.; Garcia, O.; Cobos, J.A.; , "New considerations in the input filter design of a three-phase buck-type PWM rectifier for aircraft applications," Energy Conversion Congress and Exposition (ECCE), 2011 IEEE , vol., no., pp.4087-4092, 17-22 Sept. 2011

[18] Hensgens, N.; Silva, M.; Oliver, J.A.; Alou, P.; Garcia, O.; Cobos, J.A.; , "Analysis and optimized design of a distributed multi-stage EMC filter for an interleaved three-phase PWM-rectifier system for aircraft applications," Applied Power Electronics Conference and Exposition (APEC), 2012 Twenty-Seventh Annual IEEE , vol., no., pp.465-470, 5-9 Feb. 2012

[19] Nussbaumer, T.; Heldwein, M.L.; Kolar, J.W.; , "Differential mode input filter design for a three-phase buck-type PWM rectifier based on modeling of the EMC test receiver," Industrial Electronics, IEEE Transactions on , vol.53, no.5, pp.1649-1661, Oct. 2006